Journal of Electronic Imaging

JElectronicImaging.org

Underwater image enhancement by dehazing and color correction

Chongyi Li
Jichang Guo

SPIE. IS&T imaging.org

Underwater image enhancement by dehazing and color correction

Chongyi Li and Jichang Guo*
Tianjin University, School of Electronic Information Engineering, Nankai District Weijing Road No. 92, Tianjin 300072, China

Abstract. Poor visibility due to the effects of light absorption and scattering is challenging for processing underwater images. We propose an approach based on dehazing and color correction algorithms for underwater image enhancement. First, a simple dehazing algorithm is applied to remove the effects of haze in the underwater image. Second, color compensation, histogram equalization, saturation, and intensity stretching are used to improve contrast, brightness, color, and visibility of the underwater image. Furthermore, bilateral filtering is utilized to address the problem of the noise caused by the physical properties of the medium and the histogram equalization algorithm. In order to evaluate the performance of the proposed approach, we compared our results with six existing methods using the subjective technique, objective technique, and color cast tests. The results show that the proposed approach outperforms the six existing methods. The enhanced images, as a result of implementing the proposed approach, are characterized by relatively genuine color, increased contrast and brightness, reduced noise level, and better visibility. *© 2015 SPIE and IS&T* [DOI: 10.1117/1.JEI.24.3.033023]

Keywords: underwater image enhancement; dehazing; color correction; contrast improvement.
Paper 14759 received Nov. 29, 2014; accepted for publication May 22, 2015; published online Jun. 22, 2015.

1 Introduction

Exploring the mysterious underwater world has attracted increasing attention in recent years. Clear images in marine environments play an extremely important role in exploring and investigating the underwater world, such as monitoring marine biodiversity, underwater rescue, detecting underwater pipeline leaks, underwater computer vision applications, and so forth. Poor visibility due to the effects of light absorption and scattering is challenging for processing underwater images. Such light absorption attenuates light energy, whereas scattering changes the propagating direction of light. These effects drastically degrade the quality of images acquired from the underwater environment, causing haze, contrast degradation, and color deviation. Therefore, underwater image enhancement is desired and meaningful.

There have been numerous research works on image enhancement. Traditional image enhancement methods and their variations, such as gray world (GW),[1] white balance (WB),[1] automatic white balance (AWB),[2] histogram equalization, adaptive histogram equalization and its variations,[3] and contrast limited adaptive histogram equalization[4] are simple, flexible, and attractive for real-world applications. Despite their effectiveness in terms of restoring terrestrial images, these methods have significant limitations for enhancing underwater images. Some techniques[5–8] use specialized hardware to enhance images. However, techniques using specialized hardware may be relatively time-consuming and expensive, and may require extra information from the underwater scenario. Narasimhan and Nayar[9,10] captured several images under different conditions for enhancing underwater images. Unfortunately, the method adopted by them requires multiple images of the same scene to be taken under different environment conditions, which is impractical for underwater image enhancement applications.

As underwater image processing is becoming a popular research topic, several specialized methods have emerged in recent years for enhancing the visibility of underwater images. Fairweather et al.[11] used contrast stretching and a Markov random field to enhance underwater sequences. The method has been proven effective at a conceptual level to help remotely operated vehicles interpret underwater oceanic scenes and clarify noisy image sequences. Chambah et al.[12] developed a color correction method based on an automatic color equalization model,[13] wherein the method is unsupervised, robust, and has local filtering properties leading to more effective results. Particularly, preliminary results from implementation of the method for fish segmentation and feature extraction are satisfying and promising. Torres-Méndez and Dudek[14] used a Markov random field to represent the relationship between a color-depleted image and a corresponding color image. Experimental results obtained from a variety of underwater scenes demonstrated the feasibility of their method. Trucco and Olmos-Antillon[15] presented a self-tuning image restoration filter based on a simplified version of the Jaffe–McGlamery[16,17] underwater image formation model. The simplified model is ideally suitable for diffuse-light imaging with limited backscatter, and qualitative tests show good performance under a variety of imaging conditions. Iqbal et al.[18] proposed an integrated color model to enhance underwater images based on slide stretching in RGB color space and HSI color space. The method helps to equalize the color contrast in the images and also addresses the problem of lighting. A few years later, Iqbal et al.[19] proposed an unsupervised color correction method for underwater image enhancement based on color balancing and contrast correction. It can produce better

*Address all correspondence to: Jichang Guo, E-mail: jcguo@tju.edu.cn

results than previous methods, including GW, white patch, and histogram equalization. Chiang and Chen[20] devised a novel systematic approach to enhance underwater images using a dehazing algorithm, to compensate for the attenuation discrepancy along the propagation path, and to take the influence of the possible presence of an artificial light source into consideration. Their results demonstrate that images with significantly enhanced visibility and superior color fidelity can be obtained by the proposed wavelength compensation and image dehazing approach. Ahlen et al.[21] presented a method to estimate a hyperspectral image from an RGB image and pointwise hyperspectral data. It is effective for correcting the color of the hyperspectral underwater images. The Ancuti et al. method[22] was based on fusion principles. They defined two inputs that represent color-corrected and contrast-enhanced versions of the original underwater image, as well as four weight maps that are aimed to increase the visibility of the distant objects degraded due to the medium scattering and absorption. The enhanced images and videos are characterized by a reduced noise level, better exposure of the dark regions, and improved global contrast, while the finest details and edges are enhanced. Kan et al.[23] presented a method of color restoration based on the water absorption spectrum. Considering the nonlinear attenuation of light with different wavelengths in different depths, the changes of tri-stimulus values are calculated. Some of the aforementioned methods[5,7,10,20,21] are complex and time-consuming, while some[2–4,18,19] are efficient only for specific kinds of underwater images.

In this paper, we introduce an approach to enhance underwater images based on dehazing and color correction algorithms. First, a simplified underwater hazy image formation model is used to estimate a medium transmission map and global atmospheric light. Then, the haze caused by light scattering is removed. Second, an effective color-correction algorithm is applied to further improve the visual quality of underwater images. Furthermore, in order to reduce the effects of the noise caused by the physical properties of the medium and the histogram equalization algorithm, a simple, noniterative scheme for edge-preserving smoothing (bilateral filtering) is utilized. The performance of the proposed approach is evaluated by comparing our results with the results of six existing methods using a subjective technique (by comparing visual quality), an objective technique (by comparing RGB histograms and Polar Hue Histograms), and color accuracy tests, respectively. The experimental results demonstrate that the proposed method can obtain good visual quality, superior color fidelity, good dynamic and natural shape of RGB histograms, and ideal chromatic diversity. Moreover, there is no color cast in our results.

The rest of the paper is organized as follows. Section 2 describes the proposed approach. Section 3 presents experimental results. Section 4 concludes this paper.

2 Our Enhancing Approach

In order to solve the issues discussed previously, we propose an effective and simple approach that is able to increase the visibility and restore the color balance of underwater images. Unlike existing methods, our proposed approach requires neither expensive optical instruments nor complex information about the underwater environment. Our enhancement approach consists of two main steps. In the first step, a simplified underwater hazy image formation model[24] is applied to estimate a medium transmission map and global atmospheric light. After that, the haze of underwater image is removed. In the second step, color compensation, histogram equalization, saturation, and intensity of the HSI model stretching[19] are used to increase the contrast, brightness, color, and visual quality of the underwater image. Furthermore, bilateral filtering is utilized to reduce the effects of noise. The flow chart of the proposed approach is shown in Fig. 1. The details of each step are described as follows.

2.1 *Dehazing Algorithm*

Haze is caused by light incident on objects reflected and deflected multiple times by suspended particles that exist

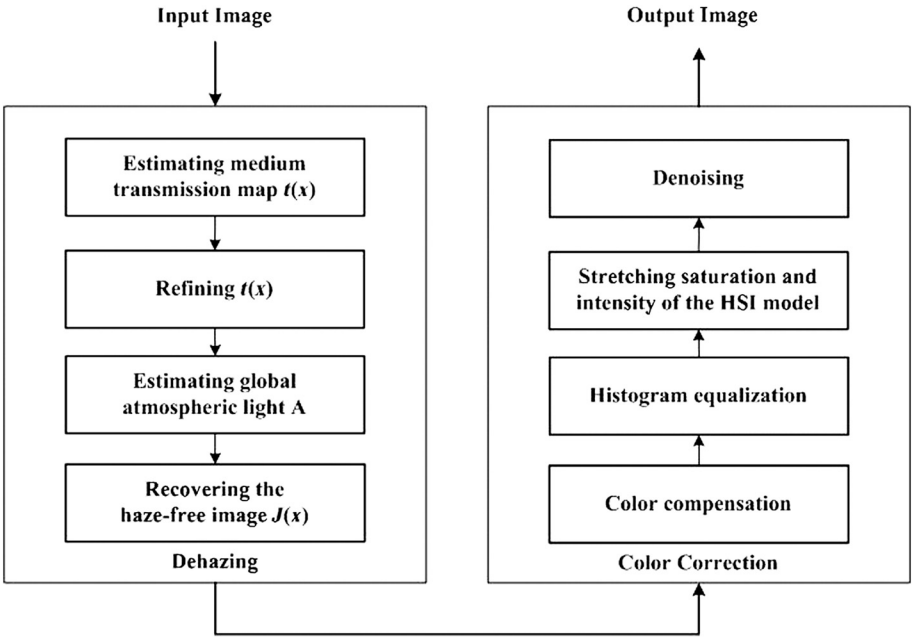

Fig. 1 Flow chart of the proposed approach.

in the water before reaching the camera. It causes low visibility and contrast of the captured underwater images. The purpose of the dehazing algorithm is to restore the clarity of underwater images. There have been a number of dehazing algorithms for outdoor images. However, most of the existing dehazing algorithms[25–27] are unsuccessful at processing underwater images. Carlevaris-Bianco et al.[28] proposed a simple, yet effective algorithm for removing the effects of haze in underwater images. Our dehazing algorithm is based on a simplified version of the Carlevaris-Bianco's algorithm.

The simplified underwater hazy image formation model can be written as

$$I(x) = J(x)t(x) + A[1 - t(x)], \tag{1}$$

where x is a pixel, $I(x)$ is the observed image, $J(x)$ is the haze-free image, A is the global atmospheric light, and $t(x)$ is the medium transmission map. $J(x)t(x)$ represents direct attenuation, which describes the scene radiance and its decay in the medium. $A[1 - t(x)]$ represents airlight, which is generated from previously scattered light and leads to the shift of the scene color. The purpose of dehazing is to restore $J(x)$, A, and $t(x)$ from $I(x)$.

The medium transmission map $t(x)$ indicates that light traveling through a transparent material will attenuate exponentially and can be calculated as

$$t(x) = \exp[-\beta d(x)], \tag{2}$$

where β is the attenuation coefficient that depends on the transmitted light wavelength, and $d(x)$ represents the scene depth.

2.1.1 *Estimating medium transmission map*

Assume that the global atmospheric light A is known. The medium transmission map can be estimated based on the fact that the red color channel attenuates much faster than the green and blue color channels. In order to determine the differences between the red color channel and the green and blue color channels, the maximum intensity of the red channel and that of the green and blue channels are compared as

$$D(x) = \max_{x\in\Omega, c\in r} I_c(x) - \max_{x\in\Omega, c\in\{b,g\}} I_c(x), \tag{3}$$

where $D(x)$ refers to the largest differences between the different color channels, $I_C(x)$ refers to a pixel x in the color channel $c \in \{r, g, b\}$ in the observed image, and Ω is a patch in the image.

The estimated medium transmission map $\tilde{t}$ can be expressed as

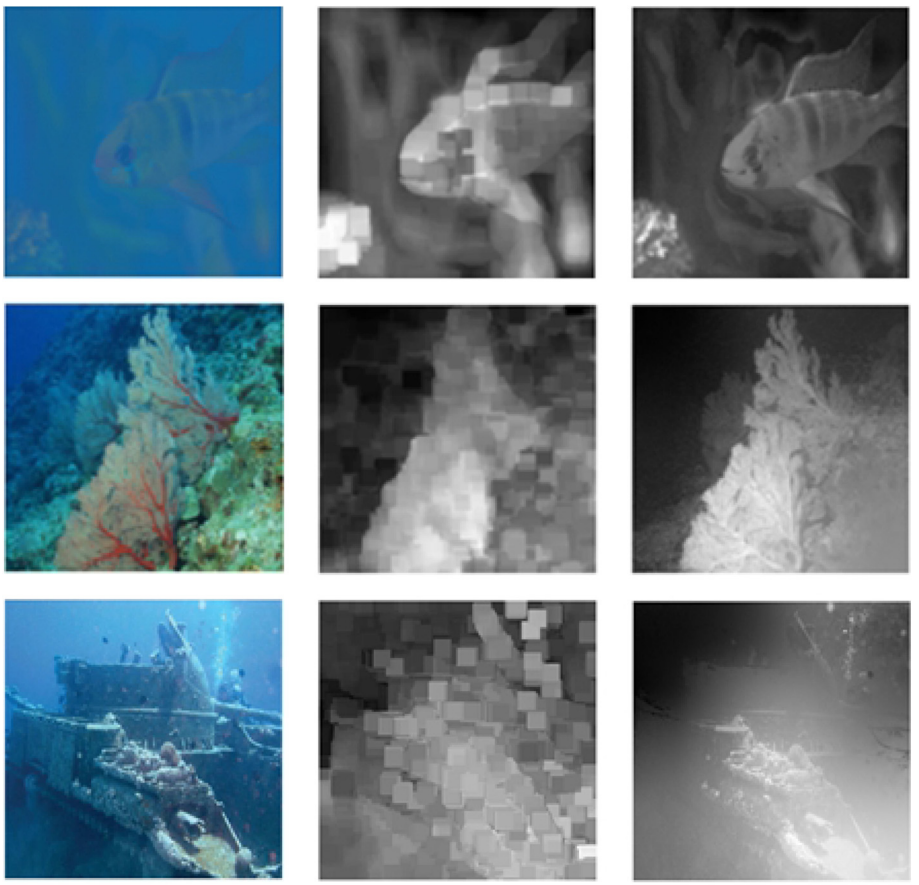

Fig. 2 Estimating medium transmission map: (a) original underwater images, (b) estimated transmission maps before applying guided filter, and (c) refined transmission maps after applying guided filter.

$$\tilde{t}(x) = D(x) + [1 - \max_{x} D(x)]. \quad (4)$$

Figure 2(a) shows three original underwater images. Figure 2(b) shows the estimated medium transmission maps [using Eq. (4)] of the original underwater images from Fig. 2(a). As can be seen, there are some halos and block artifacts in the maps of Fig. 2(b). The halos and block artifacts are produced because $D(x)$ is calculated over an image patch, which produces a coarse initial estimate of the transmission maps. Next, the He et al. guided filter[29] is applied to refine the coarse transmission maps, and Fig. 2(c) displays the refined transmission maps associated with the corresponding maps in Fig. 2(b).

In order to maintain the integrity of the images, which tend to contain a small amount of haze, and to prevent the algorithm from accentuating noise, a lower bound on the refined transmission map can be placed. It can be written as

$$\tilde{t} = \begin{cases} \tilde{t} & \text{for } \tilde{t} \geq w \\ w & \text{for } \tilde{t} < w \end{cases}, \quad (5)$$

where w is the bound. The figures in this paper were generated with the bound $w = 0.7$. The square patch size $\Omega = 31$ and the size of the image is 512×512.

2.1.2 *Estimating global atmospheric light*

The global atmospheric light can be calculated using the estimated transmission map, which has been refined by the guided filter, but has not been enforced with a lower bound yet. We determine the pixel that represents the furthest point in the image from the camera and use the intensity values at that location in the original image as the global atmospheric light. This process can be expressed as

$$\tilde{A} = I[\arg \min_{x} \tilde{t}(x)]. \quad (6)$$

2.1.3 *Recovering a haze-free image*

With the medium transmission map and the global atmospheric light now known, we can restore the haze-free image according to Eq. (1). Specifically, the haze-free image $J(x)$ can be recovered by

$$J(x) = \frac{I(x) - A}{\alpha t(x)} + A, \quad (7)$$

where $\alpha = 0.8$ is an experiential value. Figure 3 illustrates the performance of the dehazing algorithm.

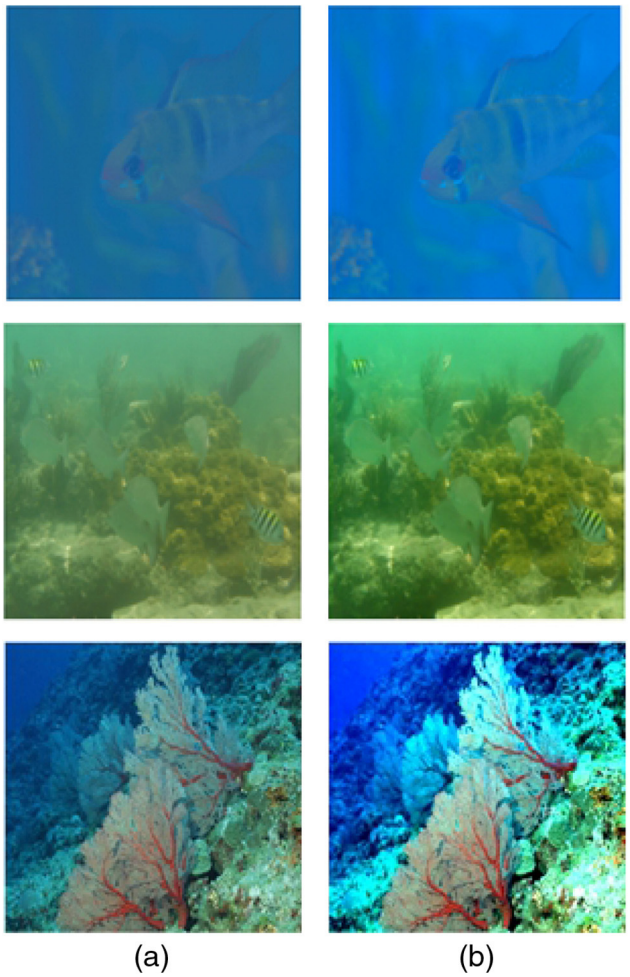

Fig. 3 Haze removal: (a) original underwater images (single fish, multiple fish_a, and coral) and (b) dehazed underwater images.

2.2 *Color Correction Algorithm*

After processing by the dehazing algorithm described previously, clarified underwater images can be obtained. Because light traveling from air to water is reflected and absorbed in the water, the underwater images are increasingly dark as the depth into the water increases. As presented by Torres-Méndez and Dudek,[14] with the increase of depth into the water, not only is the amount of light gradually reduced, but also colors drop off incrementally depending on the wavelength of the color. As a result, the underwater images show poor visibility with limited range, low contrast, blurring, and low brightness. The goal of the color-correction algorithm is to balance the color channels and to enhance color, contrast, and brightness of the underwater images. First, color compensation for each color channel is carried out to compensate for the energy attenuation caused by the physical properties of the medium. Second, histogram equalization is used to balance the color channels. Third, saturation and intensity of the HSI model stretching algorithm is applied to enhance color, contrast, and brightness. Finally, bilateral filtering is utilized to reduce noise caused by the physical properties of the medium and the histogram equalization algorithm.

2.2.1 *Color compensation*

Light with different wavelengths attenuates at different rates in water. Light of blue color travels the longest in the water because of its shortest wavelength, followed by green light and then red light. This is also the reason why underwater images tend to appear bluish. Besides, floating particles in the water can also make underwater images greenish. In order to adjust the bluish or greenish tone to a natural color, a color compensation method is utilized. In general, for every meter that a light beam passes through, the normalized residual energy ratio $\delta(\lambda)$ can be described as follows:[20]

$$\delta(\lambda) = \begin{cases} 0.8 \text{ to } 0.85 & \text{if } \lambda = 650 \text{ to } 750\ \mu\text{m} \quad \text{red} \\ 0.93 \text{ to } 0.97 & \text{if } \lambda = 490 \text{ to } 550\ \mu\text{m} \quad \text{green} \\ 0.95 \text{ to } 0.99 & \text{if } \lambda = 400 \text{ to } 490\ \mu\text{m} \quad \text{blue} \end{cases}. \quad (8)$$

According to the normalized residual energy ratio $\delta(\lambda)$, the different color channels are compensated exponentially. However, this kind of compensation is rough because an accurate depth at which the image was taken usually cannot be determined easily.

2.2.2 *Histogram equalization*

A perfect image has an equal number of pixels in all gray levels. Thus, to obtain such a perfect image, our objective is not only to spread the dynamic range, but also to generate an equal number of pixels in all gray levels. This technique is well-known as histogram equalization, which produces a uniform distribution of gray levels for the resulting image. Particularly, histogram equalization fattens and stretches the dynamic range of the histogram of the image for improving overall contrast and balancing color channels. Figure 4 shows the comparative results of the histograms before and after utilizing the dehazing and histogram equalization algorithms.

2.2.3 *Saturation and intensity of the HSI model stretching*

After histogram equalization processing, an RGB image is transformed into the HSI model, where hue (H) is a pure color component, saturation (S) is pureness of a color, and intensity (I) represents an illumination component. The algorithm of saturation and intensity of the HSI model stretching can be expressed as

$$P_O = (P_i - c)\frac{(b-a)}{d-c} + a, \quad (9)$$

where P_o is the output pixel value, P_i is the input pixel value, a is the lower limit value, b is the upper limit value, c is the minimum pixel value currently present in the image, and d is the maximum pixel value currently presented in the image.

In this paper, saturation and intensity are adjusted using Eq. (9) towards two directions (that is, downward and upward directions), and here the emphasis is placed on $(b-a)/(d-c)$, which essentially represents

$$(\text{UpperLimit} - \text{LowerLimit})/(\text{Maximum} - \text{Minimum}), \quad (10)$$

where LowerLimit $= 0$ and UpperLimit $= 255$. The aforementioned adjustments help to enhance color, contrast, and brightness of underwater images. After such a saturation and intensity process, the HSI model is transformed into an RGB image.

2.2.4 *Denoising*

To eliminate or reduce the effects of the noise, a smoothing algorithm that can remove or reduce noise while still preserving the details of the colorful underwater images that are desired. Bilateral filtering[30] is a simple, local, and noniterative scheme for edge-preserving smoothing. It can enforce the perceptual metric underlying the CIE-Lab color space, smooth color, and preserve edges in a way that is tuned to human perception. In order to test the effectiveness of the bilateral filtering for reducing noise, a comparison in terms of entropy, mean square error (MSE), and peak signal-to-noise ratio (PSNR) for the underwater images shown in Fig. 3 is performed, and the results are shown in Table 1. Because the red channel of underwater images generally is more vulnerable, the comparative results for the red channel before and after applying the bilateral filtering are shown separately in Fig. 5.

Table 1 shows the comparison among the values of entropy, MSE, and PSNR. The values representing better performance are highlighted in bold typeface. As shown in Table 1, lower MSE values, higher PSNR values, and higher entropy values are achieved after applying bilateral

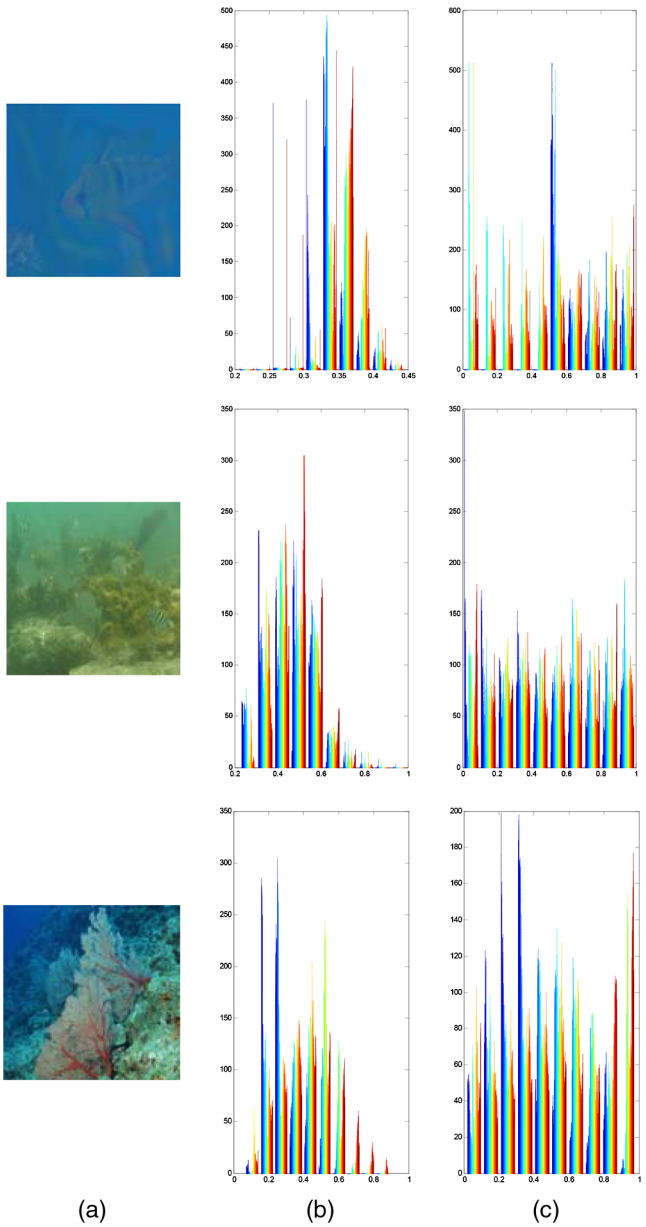

Fig. 4 Comparisons of histograms before and after utilizing the dehazing and histogram equalization algorithms: (a) original underwater images and (b) original underwater images' histograms (*x* axis is normalized color levels and *y* axis is frequency). (c) Histograms after processing by the dehazing and histogram equalization algorithms (*x* axis is normalized color levels and *y* axis is frequency).

Table 1 Comparison in terms of entropy, mean square error (MSE), and peak signal-to-noise ratio (PSNR).

Images	Method	Entropy	MSE	PSNR
Single fish	Before applying the bilateral filtering	7.5454	4.1122e + 03	11.9900
	After applying the bilateral filtering	**7.5954**	**4.0603e + 03**	**12.0452**
Multiple fish_a	Before applying the bilateral filtering	7.5829	2.9501e + 03	13.4324
	After applying the bilateral filtering	**7.7031**	**2.8623e + 03**	**13.5636**
Coral	Before applying the bilateral filtering	7.7385	2.3639e + 03	14.3945
	After applying the bilateral filtering	**7.8251**	**2.3099e + 03**	**14.4950**

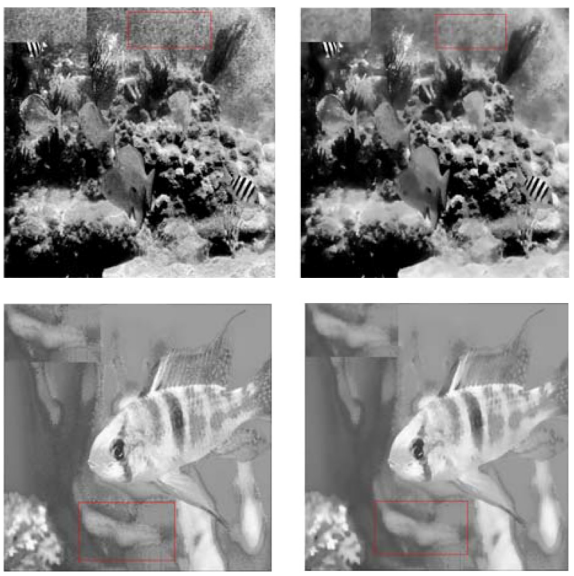

Fig. 5 Comparative results for the red channel before and after applying the bilateral filtering: (a) results for the red channel before applying the bilateral filtering and (b) results after processing by the bilateral filtering. Red rectangles indicate the details, and the amplified details can be found on the upper-left corner of each image.

filtering. Such a comparison result indicates that the bilateral filtering can effectively and sufficiently reduce noise while still preserving the valuable information of the underwater images. In addition, Fig. 5 shows that after the images are processed by bilateral filtering, the images associated with the red channel become more smooth, and the local details are enhanced. In general, Table 1 and Fig. 5 show that the bilateral filtering can effectively improve the quality of underwater images.

After color compensation, histogram equalization, saturation and intensity of the HSI model, stretching and denoising processing, clarified visibility, fine contrast and brightness, and relatively genuine color of underwater images are achieved.

3 Performance Evaluation

In order to evaluate the performance of the proposed approach, subjective evaluation (by visual inspection), objective evaluation (by comparing RGB histograms and polar hue histograms), and color accuracy tests are carried out.

3.1 *Subjective Performance Evaluation*

We compared our results with six existing methods: GW,[1] WB,[1] AWB,[2] white patch Retinex,[31] McCann Retinex,[32] and contrast limited adapt histogram equalization.[4] The results are shown in Fig. 6 and analyzed in this paper.

In this paper, we take haze, contrast, brightness, clarity, genuineness of color, and noise into full consideration. As shown in Fig. 6, our approach produces better global contrast, more genuine color, and more aesthetically pleasing image versions.

3.2 *Objective Performance Evaluation*

Since there are no underwater databases and available ground-truth images, some researchers[12,18,19] have used the RGB histograms and polar hue histograms as an analytical tool in order to evaluate the performance of their methods. We compared the results of our approach with those of the aforementioned methods using RGB histograms and polar hue histograms. The comparative results are shown in Fig. 7.

The objective evaluation technique used for the comparison adopted guidelines are derived from Ref. 12: the wider RGB histograms and more diverse chromaticity of hue histograms represent a more visually appealing image. As shown in Fig. 7, the RGB histograms of our result show better dynamic and more natural shapes, and the polar hue histograms of our result show a better chromatic diversity.

3.3 *Color Accuracy Tests*

The proposed underwater image enhancement approach based on dehazing and color-correction algorithms can also achieve friendly visual quality and superior color fidelity. In order to compare the color accuracy of our results and the results of the aforementioned methods, color accuracy tests are conducted. We adopted an effective and simple color cast detection method developed by Xiao-Zhao et al.,[33] which is based on equivalent circle and can overcome the limitation of traditional methods of detecting image color cast. According to the method, the ratio between average chroma D and chroma center distance M of image (namely color cast factor K) is applied to evaluate the level of color cast, which is expressed as

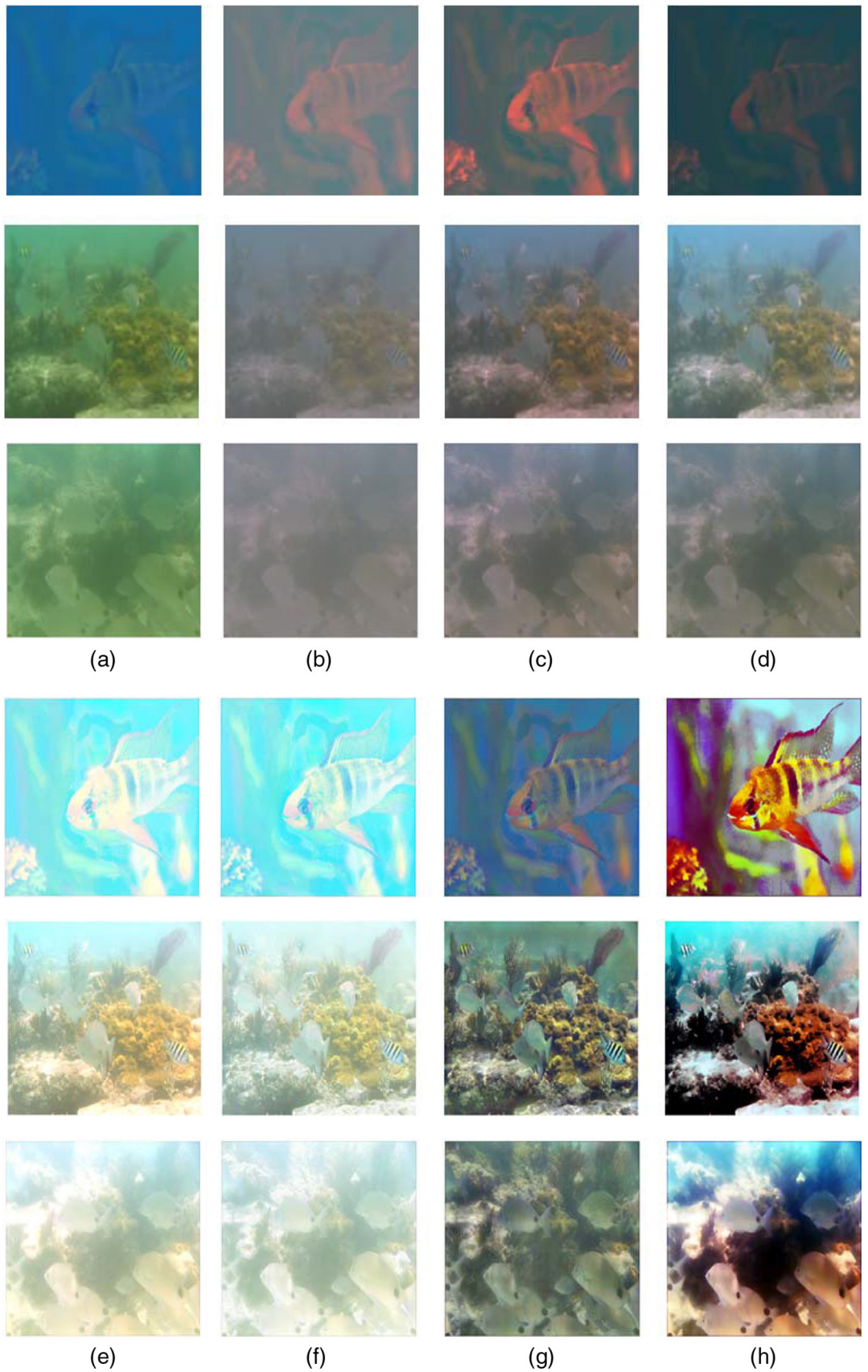

Fig. 6 Subjective comparisons of the proposed approach and the six existing methods: (a) original underwater images (single fish, multiple fish_a, and multiple_fish_b), (b) Gray World (GW)'s results, (c) white balance (WB)'s results, (d) automatic white balance (AWB)'s results, (e) white patch Retinex (WPR)'s results, (f) McCann Retinex (MCR)'s results, (g) contrast-limited adapt histogram equalization (CLAHE)'s results, and (h) results of our proposed approach.

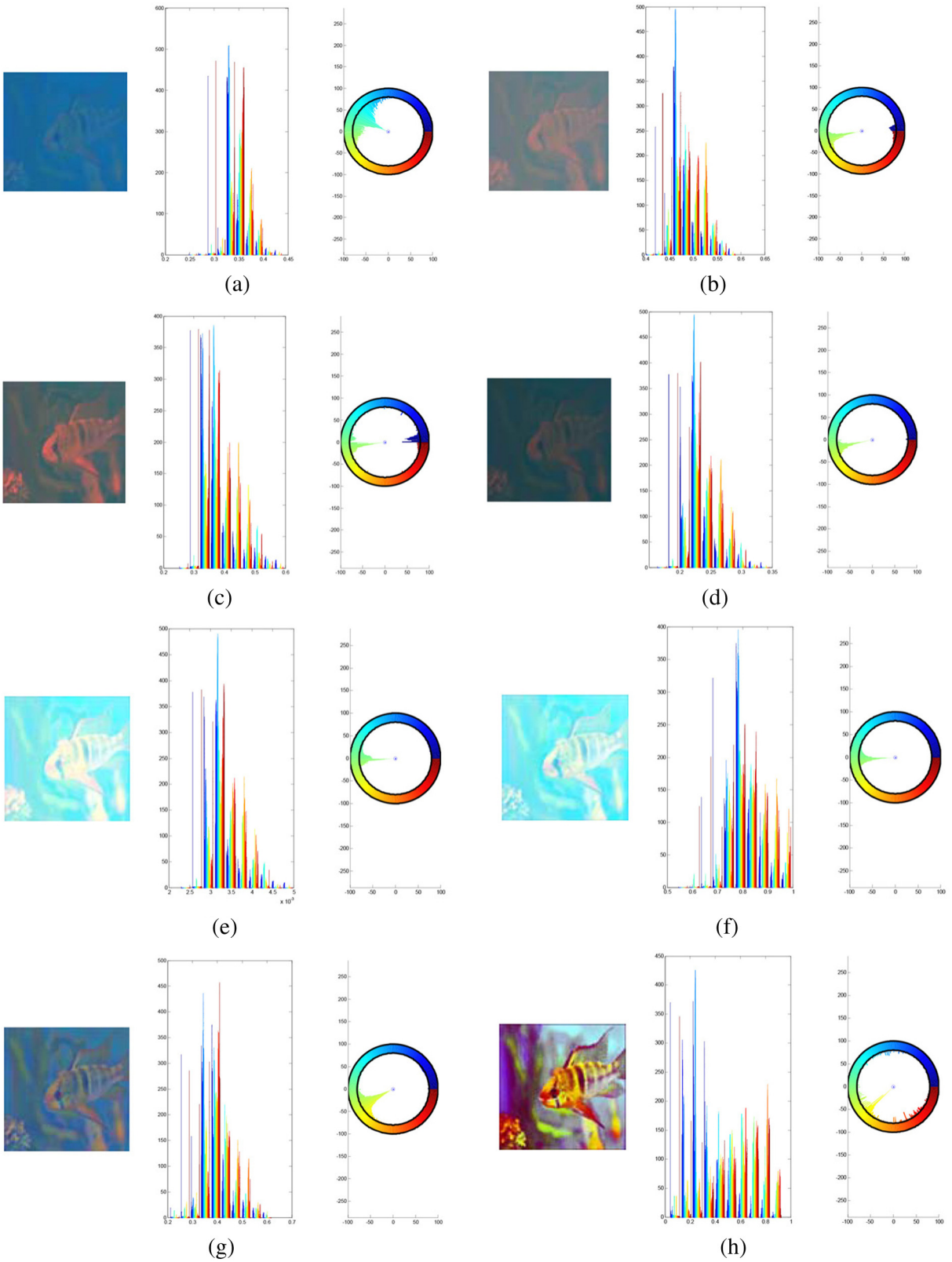

Fig. 7 Objective comparisons of the proposed approach and the six existing methods using RGB histograms (in the middle of the figures, where *x* axis is normalized color levels and *y* axis is frequency) and polar hue histograms (on the right side of the figures, where both *x* axis and *y* axis represent chromaticity). (a) Original underwater image, (b) GW's result, (c) WB's result, (d) AWB's result, (e) WPR's result, (f) MCR's result, (g) CLAHE's result, and (h) result of our proposed approach.

Table 2 Comparative values of the color cast detection.

Underwater images	Single fish	Multiple fish_a	Multiple fish_b
Color cast factor K from original images	8.755	4.453	1.175
Gray world color cast factor K	6.1605	5.7146	3.7348
White balance color cast factor K	4.2015	3.3636	3.2093
Automatic white balance color cast factor K	21.0684	4.9340	3.3632
White patch Retinex color cast factor K	10.6453	2.7818	2.8620
McCann Retinex color cast factor K	17.7076	2.8781	2.9662
Contrast limited adapt histogram equalization color cast factor K	9.6407	2.9208	2.8859
Color cast factor K from our approach	**0.434**	**0.153**	**2.7383**

$$d_a = \frac{\sum_{i=1}^{M}\sum_{j=1}^{N} a}{MN} \qquad d_b = \frac{\sum_{i=1}^{M}\sum_{j=1}^{N} b}{MN}, \tag{11}$$

$$D = \sqrt{d_a^2 + d_b^2}, \tag{12}$$

$$M_a = \frac{\sum_{i=1}^{M}\sum_{j=1}^{N} (a - d_a)^2}{MN}$$
$$M_b = \frac{\sum_{i=1}^{M}\sum_{j=1}^{N} (b - d_b)^2}{MN}, \tag{13}$$

$$M = \sqrt{M_a^2 + M_b^2}, \tag{14}$$

$$K = D/M, \tag{15}$$

where M and N are the width and height of the image, (d_a, d_b) is the center coordinate, $M = \sqrt{M_a^2 + M_b^2}$ represents the radius of the equivalent circle on the chroma $a - b$ plane in the CIE-Lab color space, and $D = \sqrt{d_a^2 + d_b^2}$ is the origin moment of the center coordinate (d_a, d_b). The level of color cast on the chroma $a - b$ plane is determined based on the location of the equivalent circle. A value of $d_a > 0$ means reddish or greenish. A value of $d_b > 0$ means yellowish or bluish. The larger the color cast factor K, the worse the color cast. In general, we define that color cast exists when K is >3. The original underwater images (single fish, multiple fish_a, and multiple fish_b) shown in Fig. 6 are used to test the color cast. Comparative values of the color cast detection are shown in Table 2.

As shown in Table 2, regardless of whether original underwater images possess color cast or not, the color cast factor K obtained from our proposed approach s are all <3; that is, no color cast. The best results are highlighted in bold typeface in Table 2. As can be seen, the proposed approach substantially outperforms all the other methods in terms of the color cast factor. One reason for the superior performance of our proposed approach is that color compensation is applied to compensate for each color channel according to different attenuation. Furthermore, the stretching of the saturation and intensity towards both directions also reduces the possibility of the color cast.

4 Conclusion

In this paper, we proposed an approach to enhance underwater images by dehazing and color correction algorithms. As discussed and illustrated, our proposed approach can effectively remove haze by implementing a simple dehazing algorithm, while obtaining good contrast and brightness, relative genuine color, and fine visibility after color correction processing. In order to evaluate the performance of the proposed approach, we compared the results of our approach with those of six existing methods using a subjective technique, an objective technique, and color accuracy tests. The results show that our proposed approach outperforms each of the six existing method. The enhanced images, as a result of implementing the proposed approach, are characterized by relatively genuine color, increased contrast and brightness, reduced noise level, and better visibility.

Acknowledgments

This research was supported by a grant from the Specialized Research Fund for the Doctoral Program of Higher Education (20120032110034).

References

1. R. Schettini and S. Corchs, "Underwater image processing: state of the art of restoration and image enhancement methods," *EURASIP J. Adv. Signal Process.* **2010**, 14 (2010).
2. C. C. Weng, H. Chen, and C. S. Fuh, "A novel automatic white balance method for digital still cameras," in *IEEE Int. Symp. on Circuits and Systems*, pp. 3801–3804 (2005).
3. S. M. Pizer et al., "Adaptive histogram equalization and its variations," *Comput. Vis., Graph. Image Process.* **39**(3), 355–368 (1987).
4. K. Zuiderveld, "Contrast limited adaptive histogram equalization," in *Graphics Gems IV*, P. S. Heckbert, Ed., pp. 474–485, Academic Press Professional, Inc., San Diego, CA (1994).
5. Y. Y. Schechner, S. G. Narasimhan, and S. K. Nayar, "Instant dehazing of images using polarization," in *Proc. of IEEE Conf. on Computer Vision and Pattern Recognition*, pp. 1–325 (2001).
6. Y. Y. Schechner, S. G. Narasimhan, and S. K. Nayar, "Polarization-based vision through haze," *Appl. Opt.* **42**(3), 511–525 (2003).
7. K. P. Pflibsen and A. N. Stuppi, "Laser light beam homogenizer and imaging lidar system incorporating same," U.S. Patent No. 5, 303, 084 (1994).

8. B. Ouyang et al., "Visualization and image enhancement for multistatic underwater laser line scan system using image-based rendering," *IEEE J. Oceanic Eng.* **38**(3), 566–580 (2013).
9. S. G. Narasimhan and S. K. Nayar, "Contrast restoration of weather degraded images," *IEEE Trans. Pattern Anal. Mach. Intell.* **25**(6), 713–724 (2003).
10. S. G. Narasimhan and S. K. Nayar, "Vision and the atmosphere," *Int. J. Comput. Vis.* **48**(3), 233–254 (2002).
11. A. J. R. Fairweather, M. A. Hodgetts, and A. R. Greig, "Robust scene interpretation of underwater image sequences," in *Proc. of IEEE 6th Int. Conf. on Image Processing and Its Applications*, pp. 660–664 (1997).
12. M. Chambah et al., "Underwater color constancy: enhancement of automatic live fish recognition," *Proc. SPIE* **5293**, 157–168 (2003).
13. A. Rizzi, C. Gatta, and D. Marini, "A new algorithm for unsupervised global and local color correction," *Pattern Recognit. Lett.* **24**(11), 1663–1677 (2003).
14. L. A. Torres-Méndez and G. Dudek, "Color correction of underwater images for aquatic robot inspection," *Lec. Notes Comput. Sci.* **3757**, 60–73 (2005).
15. E. Trucco and A. T. Olmos-Antillon, "Self-tuning underwater image restoration," *IEEE J. Oceanic Eng.* **31**(2), 511–519 (2006).
16. B. L. McGlamery, "A computer model for underwater camera systems," *Proc. SPIE* **0208**, 221–231 (1980).
17. J. S. Jaffe, "Computer modeling and the design of optimal underwater imaging systems," *IEEE J. Oceanic Eng.* **15**(2), 101–111 (1990).
18. K. Iqbal et al., "Underwater image enhancement using an integrated colour model," *IAENG Int. J. Comput. Sci.* **32**(2), 239–244 (2007).
19. K. Iqbal et al., "Enhancing the low quality images using unsupervised colour correction method," in *IEEE Int. Conf. on Systems Man and Cybernetics*, pp. 1703–1709 (2010).
20. J. Y. Chiang and Y. C. Chen, "Underwater image enhancement by wavelength compensation and dehazing," *IEEE Trans. Image Process.* **21**(4), 1756–1769 (2012).
21. J. Åhlén, D. Sundgren, and E. Bengtsson, "Application of underwater hyperspectral data for color correction purposes," *Pattern Recognit. Image Anal.* **17**(1), 170–173 (2007).
22. C. Ancuti et al., "Enhancing underwater images and videos by fusion," in *Proc. of IEEE Conf. on Computer Vision and Pattern Recognition*, pp. 81–88 (2012).
23. L. Kan et al., "Color correction of underwater images using spectral data," *Proc. SPIE* **9273**, 92730G (2014).
24. S. Q. Duntley, "Light in the sea," *JOSA* **53**(2), 214–233 (1963).
25. R. T. Tan, "Visibility in bad weather from a single image," in *Proc. of IEEE Conf. on Computer Vision and Pattern Recognition*, pp. 1–8 (2008).
26. R. Fattal, "Single image dehazing," *ACM Trans. Graph.* **27**(3), 72 (2008).
27. K. He, J. Sun, and X. Tang, "Single image haze removal using dark channel prior," *IEEE Trans. Pattern Anal. Mach. Intell.* **33**(12), 2341–2353 (2011).
28. N. Carlevaris-Bianco, A. Mohan, and R. M. Eustice, "Initial results in underwater single image dehazing," in *OCEANS*, pp. 1–8 (2010).
29. K. He, J. Sun, and X. Tang, "Guided image filtering," *IEEE Trans. Pattern Anal. Mach. Intell.* **35**(6), 1397–1409 (2013).
30. B. Zhang and J. P. Allebach, "Adaptive bilateral filter for sharpness enhancement and noise removal," *IEEE Trans. Image Process.* **17**(5), 664–678 (2008).
31. M. Ebner, "A parallel algorithm for color constancy," *J. Parallel Distrib. Comput.* **64**(1), 79–88 (2004).
32. B. Funt, J. McCann, and F. Ciurea, "Retinex in MATLAB™," *J. Electron. Imaging.* **13**(1), 48–57 (2004).
33. X. Xiao-Zhao et al., "Color cast detection and color correction methods based on image analysis," *Meas. Control Technol.* **27**(5), 10–14 (2008).

Chongyi Li is pursuing his PhD degree in the School of Electronic Information Engineering, Tianjin University, Tianjin, China. His current research focuses on digital image processing, computer vision, and especially on image enhancement.

Jichang Guo received his BS degree from Nanjing University of Science and Technology, Jiangsu, China, in 1988. He received his MS and PhD degrees in signal and information processing from the School of Electronic Information Engineering, Tianjin University, Tianjin, China, in 1993 and 2006, respectively. He is currently a full professor at Tianjin University. His current research interests include digital image processing, video coding, computer vision, and stereo video.